Absolute total electron scattering cross sections for N_2 between 0.5 and 50 eV

R. E. Kennerly*
Department of Chemistry, Indiana University, Bloomington, Indiana 47401
(Received 6 December 1979)

Absolute total electron scattering cross sections for N_2 from 0.5 to 50 eV have been measured with an estimated uncertainty of $\pm 3\%$ using a transmission time-of-flight method previously described. The results are compared to previous experimental results and to recent calculations. The positions of the $^2\Pi_g$ resonance peaks were determined with much greater accuracy (± 15 meV) than in previous transmission measurements. The structure reported by Golden (1966) below the $^2\Pi_g$ resonance was clearly not present, indicating that, if real, these features are not a property of the N_2 ground vibronic state. The shape resonance predicted at 11 eV by Dill and Dehmer (1977) was not seen, perhaps because it was too weakly manifested in the total cross section. A weak broad band centered at 25 eV may be interpreted as being due to a σ_u shape resonance as predicted by Dehmer, Siegel, Welch, and Dill.

I. INTRODUCTION

Absolute total electron scattering cross sections (TCS's) in the low-energy range are important because they are usually the most accurate absolute cross sections available. In addition, resonant scattering processes are generally very clearly seen as structure in the TCS. Total cross sections have been used extensively for normalizing various relative cross sections, modeling laser, plasma, and atmospheric processes, and stringently testing the results of theoretical calculations of the scattering process and basic atomic and molecular structures.

The relevance of such studies of N_2 is well known. Of special significance now, however, is the recent development of new theoretical methods suitable for the calculation of low-energy electron scattering processes for second-row diatomic molecules. The advantages and limitations of various models and calculational methods have yet to be thoroughly evaluated. The ability of calculated results to reproduce strongly resonant features and accurate values for the cross sections gives a clear indication of the success or failure of the model. Consequently, theoretical results are currently being critically compared with existing TCS's.[1-3] Such scrutiny has resulted in questioning of the reliability of the few available experimental results. In addition, recent experimental work has raised doubts about the reliability of the methods by which these TCS were measured.[4]

In addition to this generally unsatisfactory situation there are several specific problems which could be solved by improved measurements of the TCS. Resonant structure has been predicted[5] in N_2 which has not been observed, perhaps because of the lack of a sufficiently sensitive measurement in the appropriate energy range. Clear structure below the $^2\Pi_g$ resonance in N_2 has been observed[6] but not seen in theoretical results. The peak positions of the $^2\Pi_g$ shape resonance in integrated cross sections have been determined[7] to within ± 30 meV, but more accurate values would be useful since in model calculations the adjustment of the resonance positions is often important in the parametrization of the scattering potentials. Accurate energies would be useful to allow calibration of the electron energy scales in other transmission-type experiments.

The experimental situation for absolute differential elastic and vibrational excitation cross sections at low energy[8-10] for N_2 suggests that they are uncertain by a factor of about 2. Since the TCS can be inferred from a set of differential cross sections, the differential cross sections can be normalized or at least checked by using a reliable TCS.

The present work reports measurements of the TCS of N_2 by an accurate time-of-flight method which has been described previously.[4] These results are compared with theoretical and other experimental results, and the problems alluded to above are addressed.

II. METHOD

The method and experimental procedure for the present study were essentially those detailed by Kennerly and Bonham[4] (to be referred to as KB), which in turn refers to earlier work.[11,12] In the interest of brevity only a short description is given here. Electrons generated by a pulsed secondary-emission source were allowed to pass along a field-free path, part of which was through a gas cell. The time-of-flight (TOF) distribution of electrons from the pulsed source was recorded with and without the gas under study in the cell at a known pressure. The attenuation

as a function of the electron energy, the gas pressure, and the cell length then gave the absolute TCS by using the Beer-Lambert relation. The measurement period (about 4 h) was comprised of short (about 10 min) alternating segments with and without gas in the cell to diminish some types of possible error.

The energy resolution which has been achieved is shown in Fig. 1. The timing resolution of about 300 ps full width at half maximum (FWHM) is limiting above 5 eV. The energy resolution there is given by the expression $\Delta E(\text{meV}) \approx 0.8\, E^{3/2}$, where E is the electron energy in eV. Below this, the uncertainty due to thermal motion of the target gas[13] and the electron path length uncertainty due to the size of the secondary-emission source supercede the time-uncertainty contribution. A possible limitation at low energy, not shown in Fig. 1, is that due to the effect of surface potential variations. These would produce local changes in the energy of the electrons as they interact with the molecules in the cell and would broaden any observed resonance structure by an amount equal to these potential-energy variations, independent of the mean electron energy. For the present design and surface treatment, this contribution should be less[14,15] than 5 meV. The energy resolution shown in Fig. 1 has been obtained[12] above about 10 eV. Below this, the lack of sufficiently narrow absorption features for testing the resolution, as well as signal-to-noise deficiencies in the experiment below about 1 eV, has precluded verification of the expected behavior.

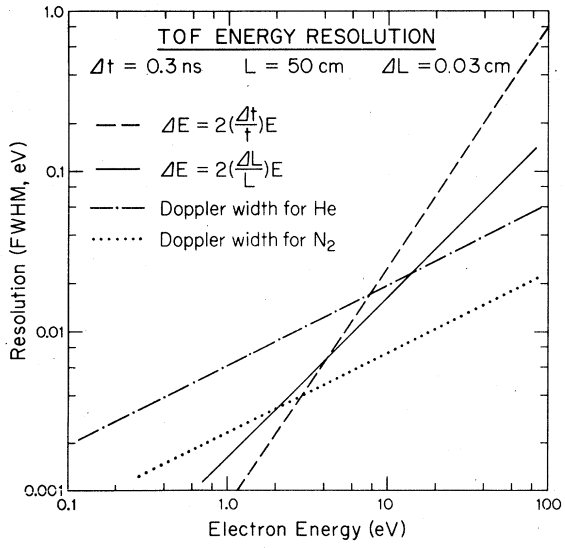

FIG. 1. Uncertainty in the energy resolution of the time-of-flight method due to uncertainties in the flight time, path length, and Doppler broadening.

Two changes of note from the apparatus of KB were made. An improved gas manifold automatically maintained the same pressure in the secondary-emission target region during both phases of the intensity measurements. This insured that there was no modification of the energy distribution of the emission due to the presence or absence of gas effusing from the scattering cell. The other change was the use of precision time-difference generators for calibration of the TOF scale, enabling highly accurate and routine energy-scale determination.

The advantages of this method over those previously existing were discussed in KB. The most important of these are the lack of pressure-dependent effects outside the scattering cell, the sufficiency of measurement at a single cell pressure, the continuous electron-energy distribution and direct and accurate energy determination, the good energy resolution, the excellent discrimination against small-angle scattering, and the basic simplicity of the method and its error evaluation.

III. ERROR EVALUATION

The error evaluation for the present case is analogous to that given in KB for the He TCS. There are some important clarifications which have since been made, however. The capacitance manometer system has been checked against a new model (MKS, Electronics 17OM-68, gauge head 310BHS-1) and was found to agree to within 0.5% in the ranges used in the present studies. This agreement has persisted for over a year, and, since one system is several years older than the other, suggests that the calibration, which is traceable to the National Bureau of Standards, was not changing significantly in time. The second gauge has permitted measurement of the thermal transpiration coefficient by the method of Baldwin and Gaerttner,[16] and it was found to be 2.0% at the pressures used in this study. (KB assumed 1%. Use of the measured value would uniformly increase these He cross sections by 1%.) Also, the pressure ratios in the three "regions" of the attenuation cell created by "baffles" have been measured and found to be less than 1%, causing a net pressure error of only about 0.1%.

Quantitative evaluations of the other error sources yielded results very similar to those for the case of He given in KB. The estimate of the sensitivity to forward scattering was judged to be less realistic in the case of N_2, however, and have doubled the error value from this source.

This gave from 2 to 3% at 50 eV depending on the aperture sizes. The total cross section error is thus estimated to be ±3% from 1 to 30 eV and ±5% elsewhere. The increase at low energy was due to increased background uncertainty.

The TOF scale was calibrated with a precision time-difference generator to better than 0.1%. Energy uncertainty from this source was therefore less than 0.2%. The only other source of energy error was due to potential differences between the cell and the remainder of the flight path. Since the cell includes about 90% of the total flight path, the difference between the actual velocity in the cell and the measured average velocity is much less than any such potential differences which may have been present. The uncertainty in energy from this effect is energy independent and less than about 10 meV.

IV. RESULTS AND DISCUSSION

The results for N_2 are shown in Figs. 2 and 3, and Table I. The number of available memory channels prevented a measurement with an adedensity of data points in the resonance region for a measurement extending over the entire range 0.5–50 eV. The TCS for lower energies in both figures was obtained from another measurement using a lower density of data points. Many measurements were performed using a range of cell pressures, aperture sizes, etc., as in KB. The reproducibility was within about 2%. The results shown in the figures are those with the least statistical uncertainties.

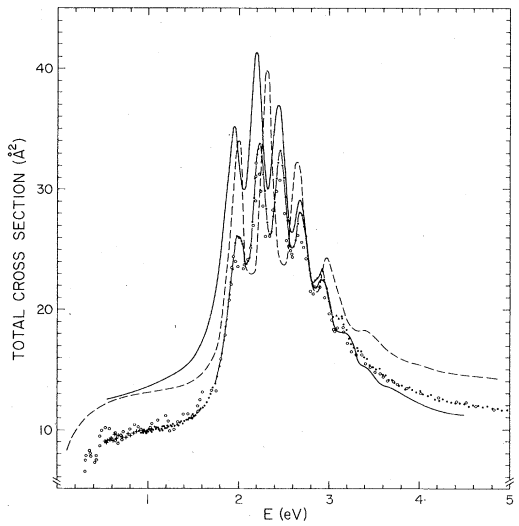

FIG. 2. $^1\pi_g$ elastic shape resonance in N_2. Present results are given by the solid circles, ●, and in the low-energy region by crosses, +, the open circles O, represent the results of Golden (Ref. 6), the solid curve, ——, is the result of the theoretical calculation of Dubé and Herzenberg (Ref. 3) and the dotted curve, ----, is the result of a theoretical calculation by Chandra and Temkin (Ref. 2).

Figure 2 shows various results in the region of the well known $^2\Pi_g$ shape resonance. This feature, first resolved by Schulz,[17] clearly dominates the low-energy cross sections. It is due to the formation of a short-lived negative-ion state by the neutral molecule and the incident electron which occupies the lowest vacant orbital,[18,19] the $^1\pi_g$ where the $l=2$ component of the $^1\pi_g$ wave function dominates; thus the resonance is described as "*d* wave" and the angular distribution of electrons ejected by the decay of the negative ion is approximately $P_2(\cos\theta)$. The lifetime of the state is about the same as the vibrational period, and the peaks result from interference between the outgoing and reflected nuclear wave functions, and thus only loosely correspond to the vibrational levels of a negative ion.[3] The complicated nature of the effect is manifested most clearly by shifts in the peaks for the different decay channels.[19] About half the decays result in vibrational excitation of the N_2 molecule. Thus vibrational excitation cross sections can be very large in the low-energy region, where the amount of direct or nonresonant excitation is extremely small.[2,20]

The magnitude of the vibrational excitation cross sections as determined by differential energy-loss measurements is at present uncertian by a factor of 2 or more.[10] The problem could be solved using a comprehensive set of relative differential cross sections to compute a relative TCS which could then be normalized with the present absolute TCS. Experimental differential cross sections of the required completeness are perhaps available,[21] but such an analysis has not been undertaken.

At higher energy where the TCS is the sum of cross sections for many processes, accurate absolute values of the TCS can supply a useful upper bound. For example, the elastic integral cross sections of Shyn, Stolarski, and Carignan[22] can be seen to be too large since they are as large as or larger than the present TCS, which includes many inelastic cross sections of considerable magnitude.[23] Similar conclusions can be drawn for a number of recent theoretical results for the elastic scattering (e.g., Ref. 5).

The present results agree well in magnitude with those of Golden[6] who employed the Ramsauer method.[24] This is somewhat surprising since numerous studies, including that of KB, suggest that the *e*-He TCS of Golden and Bandel[25] using the same apparatus, are in error by 5–10%. In

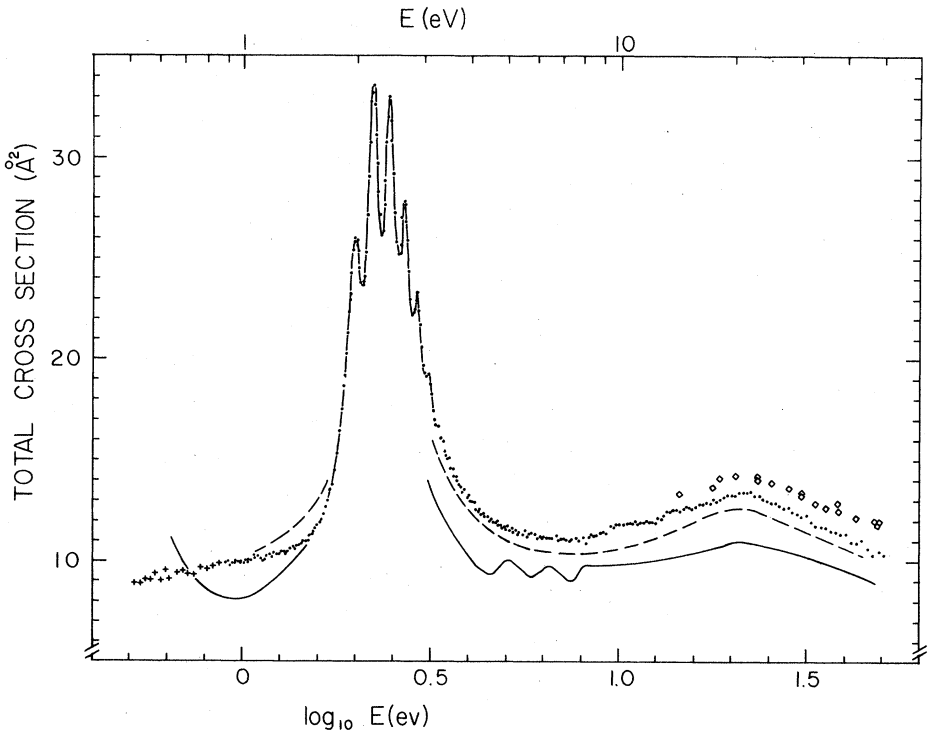

FIG. 3. The total cross section for N_2 between 0.5 and 50 eV. The solid circles, ●, and crosses +, depict the present results. The solid curve, ——, represent the results of Normand (Ref. 36) and the dashed curve, -----, those of Brüche (Ref. 37). The open diamonds represent the results of Blaauw *et al.*, but note that de Heer (Ref. 39) has advised that these results should be decreased by 5%.

the present case, the ratios of peaks to valleys in the resonance region appear to be too small for the Golden TCS, for which the stated resolution was about half the width of the peaks to be resolved. Potter *et al.*[28] suggest this and the somewhat lower magnitudes may be due in part to the presence of vibrationally excited N_2 in the Golden measurement. The resolution for the present case is about $\frac{1}{5}$ of the peak widths. We also find differences of up to 30 meV in the peak positions for the Golden results. The present peak positions have an uncertainty of ±15 meV and are given in Table II. The precise values determined by Rohr[26] for differential cross sections at three angles are of limited value for a transmission spectrum due to the large shifts in peak positions with angle and final state in the differential cross section.

No evidence is seen for the oscillatory structure seen by Golden below the shape resonance. This confirms the findings of others, both for differential[8,9] and total scattering.[27] The latter, a TOF measurement of Baldwin,[27] yields absolute values from 0.4 to 1.8 eV which are in good agreement with the present ones. Potter *et al.*[28] have suggested that the low-energy features observed by Golden were due to the buildup of a vibrationally excited population, for which the peaks would be shifted to lower energy. The present study demonstrates conclusively that such features are not due to scattering from the molecule in the ground vibrational level. However, Wong *et al.*[21] have recently observed such a shift to lower energy in scattering from a beam of vibrationally excited N_2 and have measured the cross sections for excitation to higher levels.

The theoretical situation in low-energy electron-molecule scattering has been reviewed recently by Temkin.[29] Development of the theoretical methods have advanced to the stage where accurate experimental cross sections are needed for evaluation of calculated results. TCS's are often computed and compared to experimental TCS's, the accuracy of which are usually higher than the experimental differential cross sections.

The coupled-channel results (not shown in Fig. 2) of Buckley and Burke[1] using R-matrix methods fixed the nucleii and hence showed no substructure in the resonance peak. This work extended that of Burke and Sinfailam[30] and Burke and Chandra.[31] The calculated TCS is much too large, especially in the resonance region where it has a maximum of 50 Å². Below the resonance, the results are close to the measured values. The reason for the too-large magnitudes is apparently not understood.

On the other hand, the coupled-channel calculations of Chandra and Temkin,[2] which include nuclear motion, yield a TCS which is also too large. This work used a single-center expansion

TABLE I. Present results for the N_2 total cross section.

E (eV)	σ_T (Å^2)	E (eV)	σ_T (Å^2)	E (eV)	σ_T (Å^2)
0.519	8.79	1.432	10.80	2.504	29.19
0.535	8.74	1.450	10.96	2.525	27.25
0.552	8.91	1.468	10.97	2.546	25.83
0.570	8.94	1.487	10.98	2.567	25.18
0.588	9.14	1.505	11.24	2.589	25.19
0.607	8.90	1.524	11.29	2.611	25.63
0.628	9.43	1.544	11.40	2.633	27.03
0.649	9.07	1.563	11.58	2.656	27.90
0.672	9.30	1.584	11.79	2.679	27.78
0.695	9.38	1.604	11.86	2.702	26.74
0.720	9.21	1.625	12.04	2.725	25.90
0.747	9.14	1.647	12.30	2.749	24.33
0.774	9.53	1.668	12.66	2.773	22.95
0.804	9.38	1.691	13.00	2.798	22.19
0.835	9.55	1.713	13.51	2.822	22.32
0.868	9.73	1.736	13.79	2.848	22.49
0.898	9.89	1.760	14.44	2.873	22.84
0.907	9.91	1.784	15.28	2.899	23.28
0.916	9.81	1.809	16.36	2.925	22.39
0.925	9.97	1.834	17.46	2.951	21.64
0.934	9.75	1.853	18.61	2.978	20.51
0.943	9.85	1.866	19.12	3.005	19.73
0.953	9.84	1.879	20.23	3.033	19.29
0.962	9.93	1.892	21.19	3.061	19.30
0.972	9.96	1.906	22.26	3.089	19.17
0.982	9.87	1.922	23.23	3.118	19.24
0.992	9.97	1.936	24.26	3.147	18.69
1.002	9.91	1.951	25.40	3.176	18.22
1.012	9.88	1.965	25.95	3.206	17.46
1.023	9.86	1.980	25.88	3.236	16.95
1.033	9.96	1.994	25.84	3.267	16.75
1.044	10.05	2.009	25.61	3.298	16.69
1.055	10.04	2.024	25.37	3.328	16.60
1.066	10.01	2.039	24.52	3.360	16.51
1.078	10.21	2.055	23.81	3.391	16.02
1.089	10.10	2.070	23.69	3.423	15.90
1.101	10.17	2.086	23.83	3.456	15.37
1.113	10.07	2.102	24.13	3.489	15.16
1.125	10.06	2.118	25.26	3.523	15.05
1.137	9.95	2.134	27.18	3.557	15.05
1.150	10.03	2.151	29.13	3.591	14.55
1.162	10.22	2.167	30.77	3.626	14.51
1.175	10.31	2.184	32.78	3.662	14.16
1.188	10.15	2.201	33.22	3.698	14.14
1.202	10.14	2.219	33.58	3.734	13.86
1.215	10.34	2.236	32.62	3.772	13.71
1.229	10.27	2.254	31.11	3.809	13.63
1.243	10.33	2.272	29.75	3.848	13.34
1.258	10.32	2.290	28.32	3.886	13.50
1.272	10.43	2.308	27.14	3.926	13.31
1.287	10.42	2.326	26.19	3.966	13.09
1.302	10.31	2.345	26.36	4.007	13.21
1.317	10.44	2.364	27.64	4.048	12.92
1.333	10.36	2.383	28.82	4.090	12.89
1.349	10.61	2.403	30.79	4.132	12.88
1.365	10.66	2.422	32.06	4.176	12.48
1.381	10.55	2.442	33.03	4.220	12.44
1.398	10.75	2.463	31.80	4.264	12.54
1.415	10.76	2.483	30.85	4.310	12.34

TABLE I. *(Continued.)*

E (eV)	σ_T (Å^2)	E (eV)	σ_T (Å^2)	E (eV)	σ_T (Å^2)
4.356	12.31	7.434	10.99	15.45	12.63
4.402	12.25	7.538	11.08	15.76	12.58
4.450	12.19	7.645	10.97	16.09	12.65
4.498	12.15	7.754	11.11	16.42	12.78
4.547	11.95	7.866	11.00	16.77	12.80
4.597	12.00	7.980	11.01	17.13	12.88
4.648	11.99	8.096	11.18	17.49	12.84
4.700	11.89	8.215	10.88	17.87	13.07
4.752	11.90	8.337	11.18	18.26	12.92
4.806	11.79	8.461	11.30	18.67	13.02
4.860	11.74	8.588	11.25	19.09	13.13
4.915	11.64	8.718	11.26	19.52	13.24
4.971	11.63	8.851	11.31	19.97	13.25
5.028	11.56	8.987	11.41	20.43	13.23
5.086	11.71	9.126	11.44	20.91	13.35
5.146	11.49	9.269	11.40	21.41	13.39
5.206	11.60	9.415	11.47	21.92	13.36
5.267	11.44	9.564	11.71	22.46	13.40
5.329	11.49	9.717	11.69	23.01	13.21
5.393	11.25	9.874	11.78	23.59	13.20
5.457	11.39	10.03	11.79	24.18	13.04
5.523	11.36	10.20	11.83	24.80	12.96
5.590	11.29	10.37	11.79	25.44	12.86
5.658	11.47	10.54	11.82	26.11	12.83
5.727	11.19	10.72	11.86	26.80	12.76
5.798	11.35	10.90	11.86	27.53	12.60
5.870	11.36	11.08	11.93	28.28	12.63
5.943	11.25	11.27	11.81	29.06	12.41
6.018	11.27	11.47	11.89	29.88	12.33
6.094	11.11	11.67	11.91	30.73	12.19
6.172	11.15	11.88	11.95	31.62	12.24
6.251	11.15	12.09	11.93	32.55	11.91
6.331	11.09	12.31	11.97	33.52	11.73
6.414	11.15	12.53	11.86	34.53	11.67
6.497	11.12	12.76	12.13	35.59	11.65
6.583	11.10	13.00	12.07	36.70	11.48
6.670	11.12	13.24	12.24	37.86	11.41
6.759	11.11	13.49	12.43	39.07	11.35
6.849	11.23	13.74	12.43	40.35	11.32
6.942	11.02	14.01	12.54	41.69	10.93
7.036	11.06	14.28	12.56	43.10	10.90
7.133	11.08	14.56	12.50	44.58	11.02
7.231	11.05	14.85	12.58	46.14	10.60
7.331	11.05	15.14	12.69	47.78	10.27
				49.51	10.45
				51.33	10.27

and close coupling with respect to vibration in the resonant π_g channel only. The polarization potential cutoff parameter was adjusted to position the resonance, but as can be seen in Fig. 2, the match among the calculated and measured peak positions and spacings is poor due to the coupling of a limited number of angular momentum and vibrational states.

An alternative approach has been the "compound-state" or "boomerang" model of Herzenberg and co-workers[3,32-34] which focuses on the temporary negative ion in the resonant state. The treatment uses only one partial wave and hence convergence is more readily obtained. However, the calculation is heavily parametrized (and hence relies to some extent on experimental observations of the resonance), and only resonant scattering can be treated. The latter precludes calculation of elastic scattering for N_2, which is largely nonresonant. For the purpose of comparison with an experimental TCS, Dubé and Herzenberg[3] have used the nonresonant elastic

TABLE II. π_g resonance peak positions from the present measurement. Uncertainty in the absolute energy is ±15 meV for the first four peaks, while the uncertainty in relative positions or spacings is less, being limited by the uncertainty in defining the peak centers.

Peak number	1	2	3	4	5	6	7
Energy (eV)	1.980	2.210	2.440	2.665	2.900	3.120	3.345

results of Chandra and Temkin[2] to calculate the TCS shown in Fig. 2. The agreement in the positions and shapes of the resonant features is good. This is in accord with the results of Birtwistle and Herzenberg[33] for the vibrational excitation cross sections, which are almost purely resonant and can thus be calculated entirely within the compount-state formalism. The magnitude of the TCS below about 2.5 eV is again too large but since the hybrid theory results from which the elastic values were taken are too large (see Fig. 2) this might be expected. Above 3 eV, the TCS is too small, however.

The broad maximum in the TCS around 20 eV is not well understood. Pavlovic *et al.*[34] have found a very broad peak in the vibrational excitation cross sections at 22 eV. No substructure was found at high resolution so that it was not possible to infer how many, if any, reasonances were involved. Dill and Dehmer[5,35] in a model calculation of elastic scattering found similar behavior in this energy range. Many core-excited resonance which could lead to vibrational excitation are known in this region.[19] There are also many electronic excitation channels opening which could lead to a broad enhancement in the TCS.[23]

The above-mentioned model calculation of Dill and Dehmer[5] has predicted two weak shape resonances at 11 and 21 eV which are clearly apparent in the calculated integral cross section. These features have apparently not been observed experimentally. The present results show no clear evidence for the existence of the 11-eV resonance. Faint structure can be seen around 11 eV, but this region is rich in known core-excited resonances.[19] If the predicted feature exists, it is less prominent in the TCS than in the calculated integral elastic cross section. The authors asserted however that this feature would be more readily apparent in the differential cross section.

Dehmer, Siegel, Welch, and Dill[42] have recently pointed out the existence of a broad shape resonance centered about 25 eV of σ_u symmetry which appears to account for most of the area under the broad peak at the same energy observed in this work.

The present results are compared with those of Normand,[36] Brüche,[37] and Blaauw *et al.*[38] in Fig. 3. The TCS of Brüche is quite good, which is consistent with similar comparisons[4] for He. The Normand result is generally much too small with spurious structure and incorrect shape at low energy. These two results did not resolve the vibrational structure.

The recent measurements by Blaauw *et al.*[38] from 15 to 750 eV are shown where they overlap the range of the present results. The agreement in shape is excellent but the magnitudes differ by about 7%. This difference is consistent with that found by KB[4] for He. De Heer and co-workers[39] have reevaluated the effective cell length for their apparatus and have concluded that the values reported in Blaauw *et al.*[38] and shown in Fig. 3 should be reduced[39] by 5%. Such a correction would bring them into agreement with the present results.

The molecular-beam-recoil results of Aberth, Sunshine, and Bederson[40] from 1 to 25 eV are generally about 15% too large where they overlap the present results. This error is consistent with that found by the authors for similar measurements[41] for O_2.

ACKNOWLEDGMENT

This is Contribution No. 3376 from the Chemical Laboratories of Indiana University. This research was supported in part by the National Science Foundation Grant No. GP-41983X, and also the Donors of the Petroleum Research Fund, administered by the American Chemical Society. The author wishes to thank Dr. Warren Wilson and Mr. Robert Jones for the checks and measurements involving the second capacitance manometer.

*Present address: Joint Institute for Laboratory Astrophysics, Univ. of Colorado, Boulder, Col. 80309.

[1]B. D. Buckley and P. G. Burke, J. Phys. B 10, 725 (1977).
[2]N. Chandra and A. Temkin, Phys. Rev. A 13, 188 (1976).
[3]L. Dubé and A. Herzenberg, Phys. Rev. A 20, 194 (1979).
[4]R. E. Kennerly and R. A. Bonham, Phys. Rev. A 17, 1844 (1978).
[5]D. Dill and J. L. Dehmer, Phys. Rev. A 16, 1423 (1977).
[6]D. E. Golden, Phys. Rev. Lett. 17, 847 (1966).
[7]J. A. Michejda and P. D. Burrow, Chem. Phys. Lett. 42, 223 (1976).
[8]G. J. Schulz, Phys. Rev. 135, A988 (1964).
[9]H. Erhardt and K. Willmann, Z. Phys. 204, 462 (1967).
[10]M. J. W. Boness and G. J. Schulz, Phys. Rev. A 8, 2883 (1973).
[11]R. E. Kennerly and R. A. Bonham, Chem. Phys. Lett. 43, 245 (1976).
[12]R. E. Kennerly, Rev. Sci. Instrum. 48, 1682 (1977).
[13]P. J. Chantry, J. Chem. Phys. 55, 2746 (1971).
[14]J. E. Land and W. Raith, Phys. Rev. Lett. 30, 193 (1973).
[15]F. C. Witteborn and W. M. Fairbank, Rev. Sci. Instrum. 48, 1 (1977).
[16]G. C. Baldwin and N. R. Gaerttner, J. Vac. Sci. Technol. 10, 215 (1973).
[17]G. J. Schulz, Phys. Rev. 125, 229 (1961).
[18]H. Krauss and F. H. Mies, Phys. Rev. A 1, 1592 (1970).
[19]G. J. Schulz, Rev. Mod. Phys. 45, 423 (1973).
[20]D. E. Golden, N. F. Lane, A. Temkin, and E. Gerjuoy, Rev. Mod. Phys. 43, 642 (1971).
[21]S. F. Wong, J. A. Michejda, and A. Stomatovic (unpublished).
[22]T. W. Shyn, R. S. Stolarski, and G. R. Carignan, Phys. Rev. A 6, 1002 (1972).
[23]D. C. Cartwright, S. Trajmer, A. Chutjian, and W. Williams, Phys. Rev. A 16, 1041 (1977).
[24]C. Ramsauer, Ann. Phys. (Leipzig) 66, 546 (1921).
[25]D. E. Golden and H. W. Bandel, Phys. Rev. 138, A14 (1965).
[26]K. Rohr, J. Phys. B 10, 2215 (1977).
[27]G. C. Baldwin, Phys. Rev. A 9, 1225 (1974).
[28]J. E. Potter, N. C. Steph, P. H. Dwivedi, and D. E. Golden, J. Chem. Phys. 12, 5557 (1977).
[29]A. Temkin, Comments Atom. Mol. Phys. 5, 55 (1976).
[30]P. G. Burke and A. L. Sinfailam, J. Phys. B 3, 641 (1970).
[31]P. G. Burke and N. Chandra, J. Phys. B 5, 1696 (1972).
[32]A. Herzenberg, J. Phys. B 1, 548 (1968).
[33]D. T. Birtwistle and A. Herzenberg, J. Phys. B 4, 53 (1971).
[34]Z. Pavlovic, M. J. W. Boness, A. Herzenberg, and G. J. Schulz, Phys. Rev. A 6, 676 (1972).
[35]J. Siegel, D. Dill, and J. L. Dehmer, Phys. Rev. A 17, 2106 (1978).
[36]C. E. Normand, Phys. Rev. 35, 1217 (1930).
[37]E. Brüche, Ann. Phys. (Leipzig) 82, 912 (1927).
[38]H. J. Blaauw, F. J. de Heer, R. W. Wagenaar, and D. H. Barends, J. Phys. B 10, L299 (1977).
[39]F. de Heer (private communication).
[40]W. Aberth, G. Sunshine, and B. Bederson, in *Proceedings of the Third International Conference on the Physics of Electronic and Atomic Collisions, London, 1963,* edited by M. R. C. McDowell (North-Holland, Amsterdam, 1964), p. 53.
[41]G. Sunshine, B. B. Aubrey, and B. Bederson, Phys. Rev. 154, 1 (1967).
[42]J. L. Dehmer, J. Siegel, J. Welch, and D. Dill, Phys. Rev. A 21, 101 (1980); D. Dill, J. Welch, J. L. Dehmer, and J. Siegel, Phys. Rev. Lett. 43, 1236 (1979).